Comment on "Matter-wave interferometry with helium atoms in low-*l* Rydberg states"

D. Z. Chan ⬤* and J. D. D. Martin ⬤

Department of Physics and Astronomy, University of Waterloo, Waterloo, Ontario, Canada N2L 3G1

Tommey and Hogan [Phys. Rev. A **104**, 033305 (2021)] have reported a matter-wave interference experiment using Rydberg atoms traveling through inhomogeneous electric fields at approximately 2000 m/s. Using a simplified model containing the essential physics of their experiment, we show that the phase difference measured by their observed interference fringes does not depend, in any significant way, on the acceleration of the Rydberg atoms, but instead simply on the uniform motion of the atoms through the inhomogeneous electric field.

Tommey and Hogan (TH) [1] recently reported experimental observations of matter-wave interferometry using a superposition of two Rydberg states of helium: $1s56s\,^3S_1$ and $1s57s\,^3S_1$ (hereafter *L* for lower and *U* for upper). They emphasized the importance of inhomogeneous electric fields in their experiment, which in principle cause different accelerations of the two internal states. These Stark accelerations are due to the forces that electric dipoles experience within inhomogeneous electric fields. Since the two states have different polarizabilities, they will have different dipole moments in the same electric field and thus they experience different forces and corresponding accelerations.

The purpose of this Comment is to clarify an aspect of TH's observations that might otherwise lead to misinterpretation. Specifically, we derive closed-form expressions for the phases measured by their interferograms. By numerical evaluation of these expressions, we show that their observed phases are primarily due to Stark *shifts* instead of *accelerations*, clarify the role of their large beam velocity, and briefly discuss whether their observations should be considered to be matter-wave interferometry.

The experiments performed by TH consist of repeating the following steps [see Fig. 1(a)].

Step 1. Prepare a sample of Rydberg atoms, each in state *L*.

Step 2. Form a superposition of states *L* and *U* using a resonant $\pi/2$ microwave pulse.

Step 3. Expose the atoms to a gradient electric field that causes the two internal state center-of-mass (c.m.) wave functions formed in step 2 to split.

Step 4. Apply a π pulse during a waiting period to swap the internal state of each c.m. wave function.

Step 5. Apply a second gradient pulse with the same properties as in step 3.

Step 6. Apply a resonant microwave $\pi/2$ pulse identical to step 2.

Step 7. Measure the number of Rydberg atoms in each of the two states by state-selective field ionization [2].

The microwave source should be coherent across steps 2, 4, and 6.

If we assume that the π pulse in step 4 perfectly swaps *U* and *L*, then there are two well-defined paths through this interferometer from the first to the last $\pi/2$ pulses. At the end of the sequence, one detects a mixture of *U* and *L* states that depends on the interference between these two paths. Interferograms are collected by measuring the *U*-state population $P_U = [1 - C\cos(\Delta\phi)]/2$, where *C* is the contrast,[1] as a function of an electrode potential that generates the field in steps 3 and 5. Figure 3(a) of [1] is an interferogram collected in this manner, clearly exhibiting interference fringes; however, as we will show, these fringes do not primarily depend on Stark acceleration.

Let us review how TH compute $\Delta\phi$ for the comparisons that they make with their observations. An action phase for each path ($i = 1$ or 2) is decomposed into a dynamic and a Stark phase $\phi_{\text{action},i} = \phi_{\text{dynamic},i} - \phi_{\text{Stark},i}$, with

$$\phi_{\text{dynamic},i} = \frac{m}{2\hbar}\int_0^t v_i^2 dt', \qquad (1)$$

where *m* is the mass of the helium atom and

$$\phi_{\text{Stark},i} = \frac{1}{\hbar}\int_0^t \Delta W_{S_i(t')}(t')dt', \qquad (2)$$

where $\Delta W_{S_i(t')}(t')$ is the Stark energy shift of an atom in state *S* (*U* or *L*). An explicit time dependence is given for S_i because the internal state changes at the π pulse. The separation phase is given by

$$\Delta\phi_{\text{separation}} = \frac{1}{\hbar}\left(\frac{p_1 + p_2}{2}\right)(z_1 - z_2), \qquad (3)$$

*Present address: Department of Physics and John Adams Institute for Accelerator Science, University of Oxford, Keble Road, Oxford OX1 3RH, United Kingdom; darren.chan@physics.ox.ac.uk, dzchan@uwaterloo.ca

[1]Our work here does not address the loss of contrast with increasing phase, but could be extended to address it using the same approach as TH, i.e., averaging over positions and longitudinal velocity distributions.
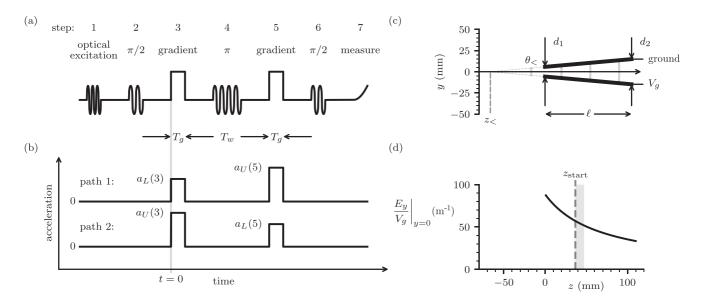
FIG. 1. (a) Steps in the interferometry experiment, where $T_g = 160$ ns and $T_w = 5000$ ns. (b) Accelerations corresponding to the two paths through the interferometer: $a_L(3)$ and $a_U(3)$ are the accelerations during the gradient pulse in step 3 and $a_L(5)$ and $a_U(5)$ are the accelerations during the gradient pulse in step 5. (c) Electrode geometry used to generate electric-field gradients in [1], with $\theta_< \approx 0.17$ rad and $z_< \approx -66.4$ mm, as determined by $d_1 = 11.5$ mm, $d_2 = 29.7$ mm, and $\ell = 105$ mm. (d) Variation in E_y along the z axis ($y = 0$), normalized by V_g (note that $E_z = 0$ along the z axis). The shaded area indicates the range of z distances that we assume the atoms to travel over from the start of first gradient pulse (step 3), $z_{\text{start}} = 36.7(10)$ mm, until the end of the second gradient pulse (step 5).

where p_i and z_i are the final computed momenta and positions for each path. The variables p_i and z_i and the integrals in Eqs. (1) and (2) are evaluated using the classical trajectories for the c.m. motion.

The final phase difference is written as

$$\Delta\phi = \Delta\phi_{\text{dynamic}} + \Delta\phi_{\text{separation}} - \Delta\phi_{\text{Stark}}, \qquad (4)$$

where $\Delta\phi_{\text{dynamic}} = \phi_{\text{dynamic},2} - \phi_{\text{dynamic},1}$ and similarly for $\Delta\phi_{\text{Stark}}$. Note that the path indices in the subtraction are in the reverse order from those in Eq. (3) [3].

In the absence of any acceleration in steps 3 and 5, it is straightforward to show that $\Delta\phi_{\text{dynamic}} + \Delta\phi_{\text{separation}} = 0$ [4]. On the other hand, if the electric field differs in steps 3 and 5, then in general $\Delta\phi_{\text{Stark}} \neq 0$, even with no acceleration during these steps. For this reason, it is helpful to define a matter-wave phase as $\Delta\phi_{\text{matter}} := \Delta\phi_{\text{dynamic}} + \Delta\phi_{\text{separation}}$, which corresponds to Stark acceleration, whereas $\Delta\phi_{\text{Stark}}$ corresponds to Stark shifts.

For instance, if steps 3 and 5 are of duration T_g with a waiting period of T_w in between [see Fig. 1(b)], then Eqs. (1) and (3) may be used to determine [4]

$$\Delta\phi_{\text{matter}} = \frac{m}{2\hbar}\left(a_g^2 - a_e^2\right)T_g^2(T_g + T_w), \qquad (5)$$

where we have assumed (i) instantaneous $\pi/2$ and π pulses and that (ii) the Stark acceleration of an atom in the L state is the same in steps 3 and 5 [$a_L(3) = a_L(5) =: a_L$] and likewise for the U state. Expressions similar to Eq. (5) are given in Refs. [5–7] for slightly different interferometry sequences.

Note that $\Delta\phi_{\text{matter}}$ as given by Eq. (5) is invariant under Galilean transformations between inertial reference frames, whereas the individual contributions $\Delta\phi_{\text{dynamic}}$ and $\Delta\phi_{\text{separation}}$ are not invariant, suggesting caution in considering them individually.

We now estimate the value of $\Delta\phi_{\text{matter}}$ using Eq. (5), by determining a_L and a_U. Accelerations are generated on atoms in state S via $\mathbf{a}_S = -[\boldsymbol{\nabla}(\Delta W_S)]/m$, where m is the mass of a helium atom. For simplicity, we will assume that the Stark shifts are quadratic in the electric-field magnitude E so that

$$\Delta W_S = -\tfrac{1}{2}\alpha_S E^2, \qquad (6)$$

where α_S is the polarizability of either the U or L state, as given by TH.

To generate an electric-field gradient, TH use two electrodes in a wedge-type configuration [see Fig. 1(c)]. As the electrodes are much wider in the $\hat{\mathbf{x}}$ direction than their separation in the $\hat{\mathbf{y}}$ direction, we may neglect any fields or variations in the $\hat{\mathbf{x}}$ direction. If for simplicity we consider only atoms moving along the z axis with $y = 0$, then in this geometry we find $\boldsymbol{\nabla}(E^2)|_{y=0} = 2(E_y\partial_z E_y)|_{y=0}\,\hat{\mathbf{z}}$.

To determine $(E_y\partial_z E_y)|_{y=0}$, we adopt a similar model to TH's, writing[2]

$$E_y|_{y=0} = \frac{V_g}{\theta_<(z - z_<)}, \qquad (7)$$

where V_g is the potential applied to the bottom electrode, the top electrode is grounded, and $\theta_<$ and $z_<$ are defined in Fig. 1(c). This approximate model may be justified by considering an infinite extension of the two electrodes in the $+\hat{\mathbf{z}}$, $-\hat{\mathbf{z}}$, $+\hat{\mathbf{x}}$, and $-\hat{\mathbf{x}}$ directions to form an infinite wedge, resulting in a two-dimensional problem in the coordinates y and z. The corresponding solution of Laplace's equation for the potential in this geometry is a standard result of complex

---

[2]To obtain TH's model, replace $\theta_<$ by $2\tan(\theta_</2)$ in Eq. (7), with a negligible difference for small $\theta_<$ such as $\theta_< \approx 0.17$ rad.

variable theory [8] and gives Eq. (7) for $E_y|_{y=0}$ along the z axis.

We now consider the time dependence of the bottom electrode voltage that determines the gradients in steps 3 and 5. Equation (5) assumes constant accelerations during the gradient pulses, whereas TH apply a time-dependent voltage to the bottom electrode [see Fig. 1(c)] by (i) linearly ramping from zero to V_g in 130 ns, (ii) holding constant V_g for 72 ns, and finally (iii) linearly ramping from V_g to zero in 130 ns. To simplify, we instead consider voltage pulses of the same value of V_g, and thus the same peak accelerations, but with negligible rise and fall times [see Fig. 1(a)]. We choose a duration of $T_g = 160$ ns to keep $\int [E_y(t)]^2\, dt$ roughly the same over each pulse as in [1], allowing us to compare Stark phases with those of TH. With the field model of Eq. (7), we find the state-dependent accelerations

$$\mathbf{a}_S = -V_g^2 \frac{\alpha_S}{m} \frac{1}{(z - z_<)} \left(\frac{E_y|_{y=0}}{V_g} \right)^2 \hat{\mathbf{z}}, \qquad (8)$$

with $E_y|_{y=0}/V_g$ depending solely on z and the geometry of the electrodes, as illustrated in Fig. 1(d).

Not all of the atoms have the same trajectories due to their different initial velocities, and the finite duration and spatial extent of the optical excitation in step 1. We focus on the trajectory of an atom with the average initial beam velocity of $v_{\text{beam}} = 2000$ m/s. Since $E_y|_{y=0}/V_g$ varies along the z axis, we need a model to determine where this atom is along the z axis at any point in the experimental sequence. Since the accelerations are weak (discussed below), we take $z = z_{\text{start}} + v_{\text{beam}}t$, estimating that $z_{\text{start}} \approx 36.7(10)$ mm at the start of the first gradient pulse, which we define as $t = 0$. (We assume that the location of optical excitation is the same as that given in Ref. [9].)

At $t = 0$, we find that $\mathbf{a}_{56s}/V_g^2 \approx -660$ m/(s^2 V^2)$\hat{\mathbf{z}}$, and thus over the approximately 160-ns duration of a $V_g = 1$ V gradient pulse, the atoms would only change velocity by $\Delta v_z \approx -e - 4$ m/s, which is small in magnitude compared to $v_{\text{beam}} = 2000$ m/s.

We now have the information required to estimate $\Delta\phi_{\text{matter}}$ as given by Eq. (5). If we model a_L as the average of $a_L(3)$ and $a_L(5)$ [Eq. (8) evaluated at the midpoints of each of the gradient pulses], and similarly for a_U, we find that $(a_L^2 - a_U^2)/V_g^4 \approx -1.0 \times 10^5$ m^2/(s^4 V^4). From Eq. (5) we may estimate $\Delta\phi_{\text{matter}}/2\pi \approx -3 \times 10^{-5}$ for $V_g \approx 4.5$ V, which is the largest V_g in the example interferogram of Fig. 3(a) of TH. In contrast, by counting fringes in this interferogram, we estimate $\Delta\phi/2\pi \approx 11$ for $V_g \approx 4.5$ V.

In using Eq. (5) we have assumed that $a_L(3) = a_L(5)$ and $a_U(3) = a_U(5)$ [see Fig. 1(b)]. However, because of the position dependence of $(E_y\partial_z E_y)|_{y=0}$ and the motion of the atoms, these accelerations cannot be equal during both gradient pulses (or even within a gradient pulse). However, introducing differing accelerations for the two gradient pulses does not significantly change the estimate for $\Delta\phi_{\text{matter}}$. Defining f so that $a_L(5) = (1 + f)a_L(3)$ and $a_U(5) = (1 + f)a_U(3)$, we find that the $T_g + T_w$ factor on the right-hand side of Eq. (5) should be replaced by $[T_g(1 + \frac{2}{3}f - \frac{1}{6}f^2) + T_w(1 + f)]$, which reduces to $T_g + T_w$ when $f = 0$ (as required). Using the field and acceleration models (7) and (8), respectively,

together with assumed motion of the atoms, we estimate $f \approx -0.25$, not significantly changing our small estimate for $|\Delta\phi_{\text{matter}}|$.[3]

A small fractional change in $|\Delta\phi_{\text{matter}}|$ is also obtained if we consider the two gradient pulses to have slightly different durations [4]. Likewise, it is not expected that our idealization of TH's gradient pulses changes $|\Delta\phi_{\text{matter}}|$ significantly.

In principle, TH's interferograms measure $\Delta\phi = \Delta\phi_{\text{matter}} + \Delta\phi_{\text{Stark}}$. In practice, given our estimate of a negligible $|\Delta\phi_{\text{matter}}|$ and the observed signal to noise ratio, TH's interferograms measure $\Delta\phi_{\text{Stark}}$, which we now estimate. For a nonzero $\Delta\phi_{\text{Stark}}$, it is sufficient that the electric fields experienced during steps 3 and 5 differ: A field gradient during steps 3 and 5 is *not* required for a nonzero Stark phase. Thus, we use the field magnitudes computed at the midpoint of the two gradient pulses, calling them $E(3)$ and $E(5)$. Using Eqs. (2) and (6), we find

$$\Delta\phi_{\text{Stark}} = -V_g^2 \frac{T_g}{2\hbar}(\alpha_U - \alpha_L)\left[\left(\frac{E(3)}{V_g} \right)^2 - \left(\frac{E(5)}{V_g} \right)^2 \right], \quad (9)$$

where $[E(3)/V_g]^2 - [E(5)/V_g]^2 \approx 5.4 \times 10^2$ m^{-2}, as evaluated using Eq. (7) and our model for the motion of the atoms during the pulse sequence.

Considering our idealizations, Eq. (9) reproduces TH's observed $\Delta\phi$ reasonably well (in the quadratic Stark shift regime). For example, from the interferogram in Fig. 3(a) of [1], we estimate that $\Delta V_g \approx 0.65(2)$ V is required to go from the central null to the first interference maxima. By setting the left-hand side of Eq. (9) to π and rearranging, we find $\Delta V_g \approx 0.62(1)$ V (where the error estimate is based on a 1-mm uncertainty in z_{start}).

The preceding analysis shows that the fringes in TH's interferograms depend primarily on inertial motion from one region of the wedge to another; Stark accelerations play an insignificant role and are not necessary to observe the interference fringes.[4] To reinforce the preceding point, imagine an experiment with atoms at rest in the laboratory, located between two parallel electrodes that generate homogeneous electric fields. The experimental sequence would be the same as that of TH [Fig. 1(a)], with the electric fields generated in steps 3 and 5 matching the values of $E(3)$ and $E(5)$ in TH's experiment for a given V_g (where the fields sampled by the atoms differ because of their motion through the inhomogeneous field). The phase measured in this hypothetical experiment would be given by Eq. (9) and thus would be the same as TH's observed phase (for a given V_g), since $|\Delta\phi_{\text{matter}}|$ is so small in comparison to $|\Delta\phi_{\text{Stark}}|$. In this hypothetical experiment, Stark acceleration is not required to observe interference. Similarly, Stark acceleration does not play a significant role in determining the phases measured by TH's interferograms.

---

[3]Variations of acceleration within each gradient pulse will be small in comparison to between pulses, due to the small gradient pulse times T_g compared to their separation T_w.

[4]The effect of the two paths sampling the field in different locations due to their different accelerations is small since, as estimated earlier, the Δv's arising from Stark acceleration (approximately equal to -10^{-4} m/s) are much smaller than $v_{\text{beam}} \approx 2000$ m/s.

A negligible $\Delta\phi_{\mathrm{matter}}$ is consistent with Fig. 3(b) of [1], which shows, at least approximately, that $\Delta\phi_{\mathrm{separation}}$ and $\Delta\phi_{\mathrm{dynamic}}$ tend to cancel. Tommey and Hogan comment on this cancellation, suggesting that it is related to the high speed that their atoms have in the laboratory frame and that lower speeds may be beneficial. However, the $\Delta\phi_{\mathrm{matter}}$ expression given by Eq. (5) is independent of any initial motion that the atoms have in the $\hat{\mathbf{z}}$ direction. (A nonzero initial v_z is assumed in the derivation but cancels out of the final expression [4].) This independence suggests that, all other things being equal, it would be difficult to observe $\Delta\phi_{\mathrm{matter}} \neq 0$ in TH's experiment by simply reducing the beam velocity.

Finally, we consider the use of the adjective "matter-wave" to describe TH's experiments. Tommey and Hogan observe interference fringes with increasing phase until the separation of the wave packets due to Stark acceleration is roughly $|\Delta z| \approx 0.75$ nm. They compare this separation with the mean de Broglie wavelength of the atoms in the laboratory frame λ_{dB}, finding that $|\Delta z| \approx 15\lambda_{\mathrm{dB}}$. However, by a Galilean transformation into an inertial reference frame in which the atoms move more slowly, λ_{dB} can be arbitrarily lengthened, exceeding $|\Delta z|$, which remains unchanged. As such, $|\Delta z| \gtrsim \lambda_{\mathrm{dB}}$ is not a criterion for matter-wave interferometry.

Alternately, one may compare the separation $|\Delta z|$ to the thermal de Broglie wavelength λ_{th} in the (mean) rest frame of the atoms. For a classical gas, λ_{th} is the coherence length for interference between spatially separated parts of a wave function [10]. For TH's experiment $\lambda_{\mathrm{th}} \approx 0.8$ nm,[5] which is close to $|\Delta z| \approx 0.75$ nm, suggesting that although Stark acceleration is not required for observation of the fringes, it may be responsible for their disappearance with increasing phase.

Thus, whether or not one considers TH's experiment to be a demonstration of matter-wave interferometry might depend on how one thinks Stark acceleration should impact TH's interferograms. It is not unreasonable to expect that a matter-wave interferometer should produce measurements that depend on the existence of two distinct paths through space-time (in this case created by Stark acceleration). In this Comment, we have demonstrated that the phases measured in TH's interferograms do not depend on there being two distinct paths through space-time. (That the paths slightly differ hardly matters.[6]) On the other hand, since $|\Delta z| \approx \lambda_{\mathrm{th}}$ the reduction in the contrast of TH's interferograms with increasing phase is possibly due to the existence of two paths.

In summary, by deriving analytical expressions for the phases measured by TH's interferograms, we have shown that Stark accelerations [Eq. (5)] make a numerically negligible contribution to their measured phases, whereas Stark shifts [Eq. (9)] dominate. Similar considerations may apply to the Rydberg atom interferometry experiment reported in Ref. [9].

---

[5]Tommey and Hogan's simulations sample from the z-axis velocity distribution with a standard deviation of $\sigma = 50$ m/s, as determined by time-of-flight measurements. This distribution corresponds to a temperature of $T = m\sigma^2/k_B \approx 1.2$ K, so $\lambda_{\mathrm{th}} = \sqrt{2\pi\hbar^2/mk_BT} \approx 0.8$ nm.

[6]A similar situation is as follows. Imagine a conventional Ramsey interferometer, with no accelerations as normal. Then suppose field gradients are introduced which cause the two internal states to accelerate slightly differently. Unless these accelerations are noticeable in the phases measured by the interferograms, one would not refer to this Ramsey interferometer as a matter-wave interferometer.

---

[1] J. D. R. Tommey and S. D. Hogan, Phys. Rev. A **104**, 033305 (2021).

[2] D. M. Walker, A. A. Morgan, and S. D. Hogan, Appl. Phys. Lett. **117**, 204001 (2020).

[3] J. M. Hogan, D. M. S. Johnson, and M. A. Kasevich, in *Atom Optics and Space Physics*, *Proceedings of the International School of Physics "Enrico Fermi,"* Course CLXVIII, Varenna, 2009, edited by E. Arimondo, W. Ertmer, W. P. Schleich, and E. M. Rasel (IOS, Amsterdam, 2009), pp. 411–447.

[4] D. Z. Chan and J. D. D. Martin, TH symbolic phase calculations, https://github.com/jddmartin/th_symbolic_phase_calcs (2023).

[5] M. Zimmermann, M. A. Efremov, A. Roura, W. P. Schleich, S. A. DeSavage, J. P. Davis, A. Srinivasan, F. A. Narducci, S. A. Werner, and E. M. Rasel, Appl. Phys. B **123**, 102 (2017).

[6] O. Amit, Y. Margalit, O. Dobkowski, Z. Zhou, Y. Japha, M. Zimmermann, M. A. Efremov, F. A. Narducci, E. M. Rasel, W. P. Schleich, and R. Folman, Phys. Rev. Lett. **123**, 083601 (2019).

[7] D. Comparat, Phys. Rev. A **101**, 023606 (2020).

[8] E. B. Saff and A. D. Snider, *Fundamentals of Complex Analysis with Applications to Engineering and Science*, 3rd ed. (Prentice Hall, Upper Saddle River, 2003).

[9] J. E. Palmer and S. D. Hogan, Phys. Rev. Lett. **122**, 250404 (2019).

[10] I. Bloch, T. W. Hänsch, and T. Esslinger, Nature (London) **403**, 166 (2000).